Stacked patch antenna and hybrid beamforming network for 5G picocell applications

D. Rodríguez-Avila*, A. K. Skrivervik
Microwave and Antenna Group (MAG), École Polytechnique Fédérale de Lausanne (EPFL), Lausanne, Switzerland
*danelys.rodriguezavila@epfl.ch

***Abstract*— This paper addresses the design of an antenna array for a portable picocell station with omnidirectional coverage. The proposed solution includes a stacked patch antenna as a single radiating element of the antenna array and a hybrid beamforming network. The antenna element works at 26 GHz with a bandwidth of 20% and a gain of approximately 8.5 dB along the operational bandwidth. The antenna is fed by a suspended stripline transitioned from a waveguide. This antenna element is used to compute a 5x12-element antenna array fed by the hybrid beamforming network. Results are analytically obtained for a fixed analog beamforming network that generates a csc^2 pattern shape in elevation. Additionally, a digital beamforming network is computed to perform beamsteering for a desired set of constraints in the azimuth plane. Simulated results of the complete system yield promising insights on the capacity of the proposed design to provide omnidirectional coverage.**

***Index Terms*—picocell, stacked patch antenna, suspended stripline, beamforming, csc^2 shaped pattern, omnidirectional coverage.**

I. INTRODUCTION

In the frame of the coming mobile generation, this work aims to develop a portable picocell antenna for bringing service to a region in case of rescue, disaster or other security situations. This base station should comply with the 5G spectrum allocation and bandwidth for mm-Waves nodes. Furthermore, omnidirectional coverage in a cell radius of up to 200 m for mostly Line of Sight (LoS) links is required. In addition, the antenna should be directive to overcome the dissipation with distance and atmospheric attenuation characteristic to mm-Waves. A beamforming feeding network is thus necessary to fulfill the application requirements. However, beamforming networks for mm-Waves antenna systems with an optimal performance can only be obtained at expenses of a complex design with high power consumption and cost [1]. Therefore, we propose in this project a hybrid beamforming feeding network composed of an analog fixed network (ABFN) in elevation and a digital beamforming network (DBFN) in the azimuth plane. This network will be used to feed an antenna array of 5x12 elements, as shown in Fig. 1. In elevation, a uniform received power will be achieved by a csc^2 radiation pattern. In azimuth, a 360° coverage will be obtained by steering the beam digitally to a desired target direction, beamwidth and side lobe level constraints.

The state of the art in this context shows a number of antennas that could be used. In order to compare them according to our requirements, special attention has been given to the antenna performance (gain and bandwidth), losses, integration capacities and cost.

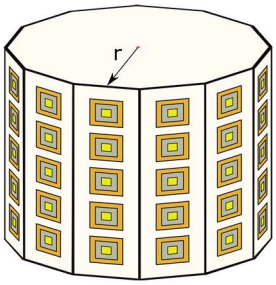

Fig. 1. Antenna array for picocell application

Printed antenna elements fed by microstrip networks were designed in [2] and [3]. Wide bandwidth and high gains were obtained; however, the intrinsic high losses of microstrip printed lines in mm-Waves reduce the scalability of these techniques for denser 5G systems. In order to avoid losses, metallic waveguide networks have also been considered but with considerable disadvantages regarding integration and cost. A very interesting low profile solution are metallic slotted waveguide antennas [4]. In 2004, Gatti et al. published a csc^2 pattern antenna where the pattern shaping was controlled through the slots offset and length. The main advantage of this prototype is that both the antenna and the feeding network are the same structure, which enables obtaining a low loss and small size antenna. However, they are also characterized by having a narrow bandwidth, difficult integration with planar structures and higher cost, which makes them less attractive in this context. Slotted waveguide antenna designs have been also implemented using planar structures. More recent designs using Substrate Integrated Waveguide (SIW) technology show promising results. High gain antennas with broader bandwidth and low side lobe levels were proposed for uniform phase array applications in [5] and [6]. Based on the same technology, different feeding networks such as Butler matrices were proposed. These configurations can be implemented with lower crossover and losses than their microstrip line counterparts [7], [8]. Even though SIW is a potential technology to be used in 5G antennas, dielectric losses and leakage energy should be carefully considered, especially for large antenna systems where the feeding networks may result in a large structure. Another interesting solution to fulfill the main mm-Waves antenna requirements are stacked patch antennas. Multilayer structures in general

are usually preferable in mm-Waves applications to overcome the high cross polarization and spurious radiation characteristics of single layer antennas. Stacked patch stripline-fed antennas were proposed in [9]–[11]. Although high gain and bandwidth were obtained, this feeding line can also lead to significant losses when larger arrays are desirable. A potential solution to this is to use suspended striplines (SSL). This type of transmission line is shielded and mounted on a thin substrate such that most of the dielectric is air. Since a quasi-TEM mode is propagated in a small effective permittivity medium, SSL present low losses and small dispersion [12]. Even if more bulky than the conventional printed lines, they represent a good compromise for broad bandwidth mm-waves solutions. Stacked patch antennas fed by SSL have been already designed for radar and satellite communications [13], [14]. In this paper, a SSL fed stacked patch antenna is presented considering the frequency band requirements of 5G antenna systems. A single element is obtained, and a hybrid beamforming feeding network is simulated analytically to evaluate the performance of this structure regarding omnidirectional coverage and adaptive beamsteering capacity. A solution for a portable picocell station that balances performance, complexity and cost is hence proposed.

II. Radiating Element

This section describes the design considerations of the stacked patch antenna element. In addition, simulated results are discussed.

Fig. 2 shows the 3D exploded view of the antenna element prototype. It is mainly composed of three structures (see Fig. 2 from right to left): the WG-to-SSL transition, the SSL line and the stacked patches layers, each of them described next. The antenna works in the 26 GHz band (24.25-27.5 GHz), which is considered by the Electronic Communication Committee (ECC) as one of the possible allocations for the 5G mobile service in Europe [15].

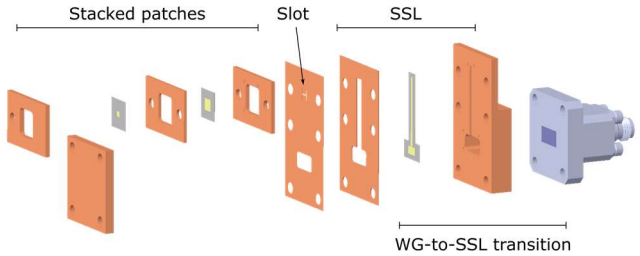

Fig. 2. Extrude view of the radiating element [color code for materials: yellow - copper, gray - substrate, orange - brass except for ground plane (beryllium), purple - connector]

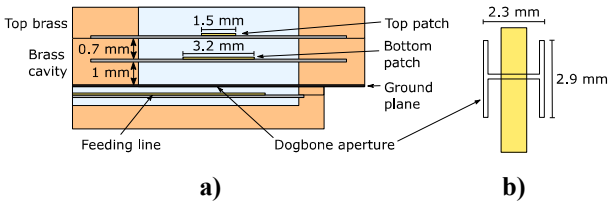

Fig. 3. Detailed dimensions of a) stuck patches and b) dogbone aperture

After considering different possible solutions to feed the SSL (e.g., direct probe feed or CPW to SSL transition), the WG-to-SSL transition was selected taking into account loss mismatches, fabrication tolerances and geometrical compatibilities. A coax-to-WR-34 adapter, whose dimensions were considered in the design, will be connected to feed the transition. The input match for the desired bandwidth is lower than -13 dB and the insertion loss is better than -0.4 dB. Dimensions such as the size of the transition patch and the WG short length were crucial in achieving those figures.

The 50 Ω SSL consists of a copper line of 0.85 mm mounted on a substrate (RT 6002) 0.127 mm high. Above and below the stripline, a 0.3 mm layer of air was kept, and the line is shielded using brass. The shielded SSL cavity is 3 mm wide to avoid higher order modes.

Energy is coupled to the patches through a dogbone aperture (see Fig. 3.b) in the ground plane, which gives significantly improved coupling and can be arranged in a smaller area than a standard rectangular slot with the same total length. Due to the symmetry of the dogbone aperture, good polarization purity is ensured [16].

The stacked patch arrangement consists of two patches mounted on low permittivity thin substrates (see Fig. 3.a). They are separated from each other and from the ground plane by hollow brass structures that allocate 1 mm (top patch) and 0.7 mm (bottom patch) air gaps. The combination of these air gaps and the substrate membranes produces a thick structure with low effective permittivity, which enables a wider band operation. The dimensions of the two patches have been tuned with this goal.

In addition, the aforementioned brass structures together with the top cavity provide a shielded boundary, which reduces mutual coupling between elements when used in antenna arrays. The top cavity dimensions were calculated to enable propagation along the operational bandwidth, yielding a minimum aperture width of 6.3 mm. This value, however, is larger than λ/2, which is a desirable distance between elements in antenna arrays. A compromise was made using a cavity width of 7.5 mm, resulting on minimum distance between elements of approximately 0.65λ. The optimized antenna results are summarized next.

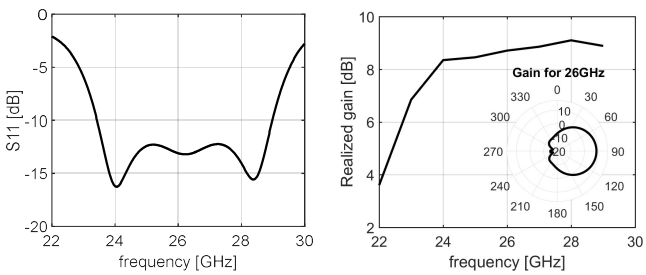

Fig. 4. Radiating element results: a) S11 b) Realized gain and gain radiation pattern for 26 GHz

The patch antenna works in 26 GHz with a bandwidth wider than 5 GHz (Fig. 4.a). The realized gain is stable for the desired frequency band, with values around 8.5 dB (Fig. 4.b).

Fig. 4.b also depicts the realized gain pattern for 26 GHz. The most critical dimensions in tuning the antenna to the design requirements were the air gap thickness, the slot length, the stub length and the patches dimensions.

III. ANALYTICAL HYBRID BEAMFORMING NETWORK

In this section, an analytical hybrid beamforming network to feed a 5x12-antenna array is proposed. It consists of two main sections: a fixed analog beamforming network in the elevation plane and a digital beamforming network to steer the beam in azimuth. The simulated radiation pattern of the antenna element obtained in Section II is used to build the antenna array. This is useful to evaluate the effectiveness of using this element to build the full antenna array system.

The 5-element linear array can be seen in Fig. 5. As mentioned before, this subarray is fed by a fixed ABFN, further detailed in Section IIIA. The 5-element subarray has been rotated and replicated 12 times to form a sectored antenna (Fig. 1). This configuration will be used to compute the DBFN weighting vectors for steering the beam in the azimuth plane. Section IIIB summarizes the main procedure and results of the DBFN design.

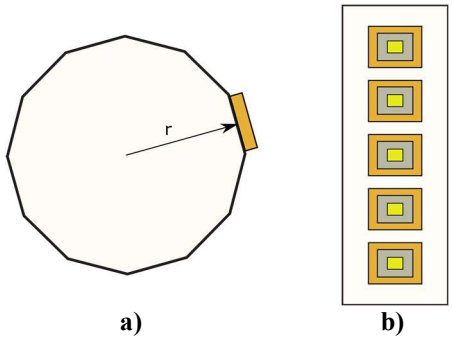

Fig. 5. 2D view of an antenna subarray a) top view b) front view

A. Analog beamforming in elevation

Using a csc^2 radiation pattern is an established solution to guarantee uniform power distribution in elevation. This shape is usually desirable in mobile communications to distribute the radiated power evenly between a maximum incident angle and the angle in the mast shadow.

In this section, the weighting vector $w_{1xN}(\theta_i,\Phi_j)$ that generates a csc^2 shape has been computed by solving a least squares problem that can written as:

$$w_0 = arg\,min_{w(\theta_i,\Phi_j)} \left\| \Delta_{\theta_i,\Phi_j} - A(\theta_i,\Phi_j) w(\theta_i,\Phi_j) \right\|^2, \quad (1)$$

where $A(\theta_i,\Phi_j)$ is the antenna array response and Δ_{θ_i,Φ_j} is the desired mask. Fig. 6 shows the obtained radiation pattern $AF_{el}(\theta_i,\Phi_j)$ compared to the ideal mask. The synthesized amplitude and phase values for the five antenna elements can be seen in Table 1.

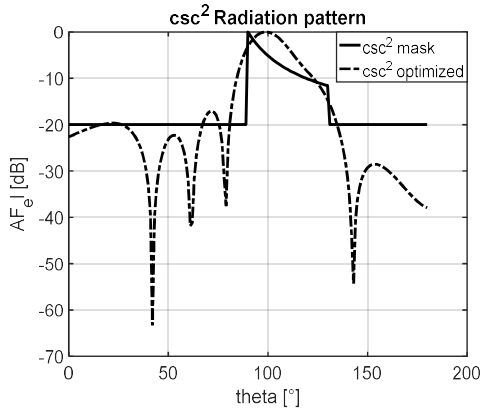

Fig. 6. 2D mask and synthesized csc2 pattern

The obtained radiation pattern covers a range of approximately 63°, which is larger than the typical range for similar applications (around 30°). This guarantees a wide uniformly distributed power in the elevation plane.

TABLE 1 SYNTHESIZED AMPLITUDE AND PHASE VALUES FOR AF_{el}

	Element #1	Element #2	Element #3	Element #4	Element #5
Amplitude [W]	0.1802	0.4208	0.2912	0.0672	0.0405
Phase [°]	105.5	47.1	-9.7	-41.5	-29.5

The obtained matrix $AF_{el}(\theta_i,\Phi_j)$ will be used to compute the azimuthal antenna array in the next subsection.

B. Digital beamforming in azimuth

The computed digital beamformer generates a matrix $U_{MxΓ}(\theta_i,\Phi_j)$ with column wise distributed weighting vectors $u_{Mx1}(\theta_i,\Phi_j)$ that fulfill a set of constraints. The first constraint C1 consists in targeting the radiation pattern maximum at a certain direction θ_i,Φ_j. In addition, the beam should cover a certain area specified by the radiation pattern beamwidth (C2). Finally, in order to provide omnidirectional coverage with directive antennas, beams should be spatially orthogonal. That is, beams could be simultaneously active but the maximum of the beam pointing at θ_i,Φ_j should overlap with the minimum of the rest of the beams. This is represented by the third constraint C3, and it will be addressed as the beam on θ_i,Φ_j having a side lobe level (SLL) below a specified threshold. The three regions defined by constraints C1, C2 and C3 are used to build the desired mask function (see Fig. 7).

This mask is used to solve a least square problem with a cost function similar to (1). The array response for this case has been built by both rotating and translating the matrix $AF_{el}(\theta_i,\Phi_j)$ obtained in the previous section. An iterative optimization process using the CVX Matlab-based modeling tool for convex optimization was used to obtain the desired weighting vectors $u_{Mx1}(\theta_i,\Phi_j)$. A fourth constraint C4 was added to this problem formulation in order to limit the network power distribution and thus minimize the number of active components in the antenna array ($C4: \|w\|_1 < 1$). The 3D mask used to solve this problem contains the desired csc^2 mask in elevation applied in section IIIA.

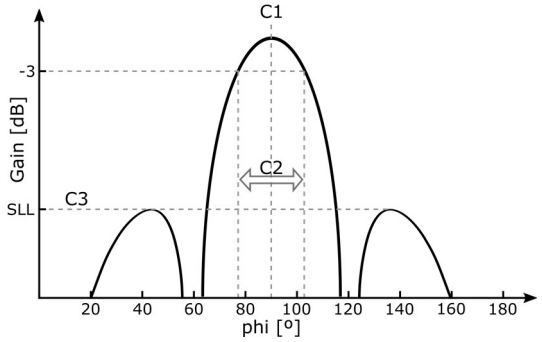

Fig. 7. Radiation pattern regions for constraints C1, C2 and C3

Fig. 8 and Fig. 9 show radiation patterns $AF_{az}(\theta_i, \Phi_j)$ computed for two set of constraints (S1 and S2), which have been selected to meet the performance requirements of the envisioned application. Due to the array symmetry, the digital beamforming network was computed to generate beams in only 1/8 of the structure. The first set S1 aims to synthesize beams targeting 90°, 105°, 120° and 135° (C1), all of them for a beamwidth of 30° (C2) and a desired SLL below -15 dB (C3). The second set S2 is defined with the same constraints C1 and C3, but a beamwidth (C2) of 50°. Results for set S1 and S2 are summarized in Fig. 8 and Fig. 9 respectively.

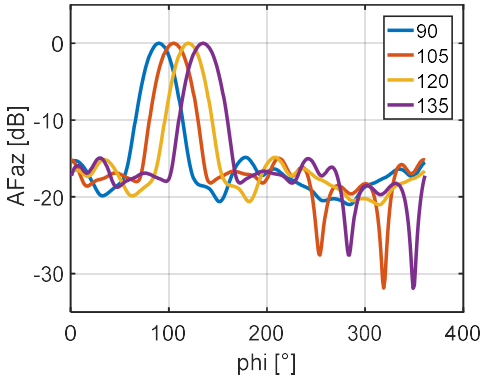

Fig. 8. Radiation patterns $\boldsymbol{AF_{az}}$ for set of constraints S1

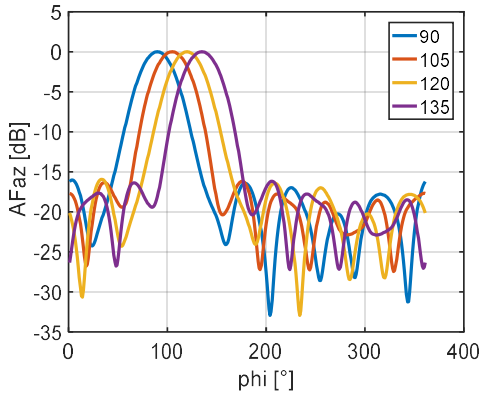

Fig. 9. Radiation patterns $\boldsymbol{AF_{az}}$ for set of constraints S2

This digital beamforming network provides a set of weighting vectors that steer the antenna beam in a range of target directions with different beamwidths and relatively low SLL. As depicted in the figures, all constraints are fulfilled in both cases, enabling omnidirectional coverage for the present application. For smaller beamwidths and lower SLL, beamsteering would require increasing the number of sectors to enhance positive interference. Resulting performance could also be improved by modifying the distance between subarrays to a value closer to λ/2. Planar arrays per sector with an optimized distance between subarrays could also be considered to overcome this limitation, although leading to a larger array and therefore a more expensive prototype.

IV. Conclusions

The design of a broadband antenna for a portable picocell station requiring omnidirectional coverage has been addressed. A stacked patch antenna working at 26 GHz is proposed for the single radiating element. Large bandwidth and high gain are obtained using a multilayer structure with air gaps between the two patches. The radiating element was shielded in order to reduce the mutual coupling when used in array configurations. This antenna is fed by a low loss and low dispersion transmission line that ends in a WG-SSL transition connector for diminishing fabrication mismatches. A 5x12-antenna array was designed using this antenna as unit radiating element. Omnidirectional coverage is achieved through a hybrid beamforming feeding network. The fixed analog beamforming network, with a $\csc^2$ beam shape in elevation, guarantees uniform received power for more than 60° below the horizon. Additionally, a weighting matrix for beamsteering and beamwidth forming with reasonably low SLL can be synthesized using the proposed digital beamforming network. With this study, the effectiveness of using the stacked patch antenna prototype as unit cell of antenna arrays fed by hybrid beamforming networks has been shown to provide promising results. This proposal represents a balanced solution for a portable picocell station considering performance, complexity and cost. Its implementation is now being undertaken for experimental validation.

V. Acknowledgment

This work was supported by Armasuisse through the project Antennas for 5G. The authors of this paper acknowledge their financial support.

VI. References

[1] X. Huang, Y. J. Guo, and J. D. Bunton, "A hybrid adaptive antenna array," IEEE Trans. Wirel. Commun., vol. 9, no. 5, pp. 1770–1779, 2010.

[2] K. Klionovski and A. Shamim, "5G Antenna Array with Wide-Angle Beam Steering and Dual Linear Polarizations," in Antennas and Propagation & USNC/URSI National Radio Science Meeting, 2017, pp. 1469–1470.

[3] Y. Rahayu and I. R. Mustofa, "Design of 2×2 MIMO Microstrip Antenna Rectangular Patch Array for 5G Wireless Communication Network," in 2017 Progress in Electromagnetics Research Symposium - Fall (PIERS - FALL), 2017, pp. 19–22.

[4] R. V. Gatti and R. Sorrentino, "Slotted waveguide antennas with arbitrary radiation pattern," in IEEE Antennas and Propagation Society Symposium, 2004, 2004, pp. 821–824.

[5] T. Mikulasek, J. Puskely, J. Lacik, and Z. Raida, "Design of

aperture-coupled microstrip patch antenna array fed by SIW for 60 GHz band," IET Microwaves, Antennas Propag., vol. 10, no. 3, pp. 288–292, 2016.

[6] W. M. Abdel-wahab, S. Member, and S. Safavi-naeini, "Wide-Bandwidth 60-GHz Aperture-Coupled Microstrip Patch Antennas (MPAs) Fed by Substrate Integrated Waveguide (SIW)," Antenna, vol. 10, no. Layer 4, pp. 1003–1005, 2011.

[7] Y. J. Cheng et al., "Substrate integrated waveguide (SIW) Rotman lens and its Ka-band multibeam array antenna applications," IEEE Trans. Antennas Propag., vol. 56, no. 8 II, pp. 2504–2513, 2008.

[8] K. Tekkouk, M. Sano, R. Sauleau, M. Ettorre, and M. Ando, "60-GHz Multi-layer Multi-beam Slotted Waveguide Array made by Diffusion Bonding Technique," 2015 9th Eur. Conf. Antennas Propag., pp. 1–4, 2015.

[9] G. L. Huang, S. G. Zhou, T. H. Chio, C. Y. D. Sim, and T. S. Yeo, "Waveguide-Stripline Series-Corporate Hybrid Feed Technique for Dual-Polarized Antenna Array Applications," IEEE Trans. Components, Packag. Manuf. Technol., vol. 7, no. 1, pp. 81–87, 2017.

[10] S. Karimkashi and G. Zhang, "A dual-polarized series-fed microstrip antenna array with very high polarization purity for weather measurements," IEEE Trans. Antennas Propag., vol. 61, no. 10, pp. 5315–5319, 2013.

[11] L. Qiu, H. Y. Qi, F. Zhao, K. Xiao, and S. L. Chai, "A Shaped-Beam Stripline-Fed Aperture-Coupled Stacked Patch Array," IEEE Trans. Antennas Propag., vol. 64, no. 7, pp. 3172–3176, 2016.

[12] T. Itoh, "Overview of Quasi-Planar Transmission Lines," IEEE Trans. Microw. Theory Tech., vol. 37, no. 2, pp. 275–280, 1989.

[13] N. Nakamoto, T. Takahashi, A. Ono, M. Nakashima, M. Ohtsuka, and H. Miyashita, "A Dual Polarized Suspended Stripline Fed Open-Ended Waveguide Antenna Subarray for Phased Arrays," in 2015 International Symposium on Antennas and Propagation (ISAP), 2015.

[14] R. Głogowski, J. F. Zurcher, J. R. Mosig, and C. Peixeiro, "Circularly polarized aperture coupled stacked patch antenna element for Ka-band," IEEE Antennas Propag. Soc. AP-S Int. Symp., pp. 911–914, 2011.

[15] P. Faris, "The road to 5G deployment- an update on ongoing harmonisation and standardisation activities," ECC Newsletter. [Online]. Available: http://apps.cept.org/eccnews/sep-2017/index.html.

[16] F. Croq and D. M. Pozar, "Millimeter-Wave Design of Wide-Band Aperture-Coupled Stacked Microstrip Antennas," IEEE Transactions on Antennas and Propagation, vol. 39, no. 12. pp. 1770–1776, 1991.